A numerical study on the interaction between friction and vibration in a friction-involved dynamical system

Journal of Physics: Conference Series **2909** (2024) 012023 doi:10.1088/1742-6596/2909/1/012023

A numerical study on the interaction between friction and vibration in a friction-involved dynamical system

Ahmad Algara[1], and Jie Yuan[1,2]

[1]Aerospace Centre of Excellence, Department of Mechanical and Aerospace Engineering, University of Strathclyde, Glasgow, G1 1XQ, United Kingdom.

[2]Department of Aeronautics and Astronautics Engineering, University of Southampton, Southampton, SO17 1BJ, United Kingdom.

The corresponding author's e-mail addresses: ahmad.algara@strath.ac.uk, j.yuan@soton.ac.uk

Abstract

Friction can be regarded as a dynamic variable within a dynamical system including sliding interfaces. In general, friction and vibration effects have been studied together in many studies but usually studied in one direction, primarily focusing on the effects of friction on vibration and other direction has not been widely studied, with limited attention given to their closed-loop feedback interactions in engineering applications. The presence of friction and contact surfaces introduces nonlinearity, affecting the system's dynamic response. Moreover, oscillations applied to these structures can influence contact mechanics at friction interfaces, particularly relevant for decommissioning large-scale structures like wind turbines. However, modelling the intricate interplay between friction and vibrations is overly complex, requiring expertise from fields such as contact mechanics, tribology, and nonlinear dynamics.

The objective of the study is to investigate the mutual influences between structural vibrations and contact friction for friction-involved dynamical systems. A two-degree-of-freedom (2-DoF) lumped-parameter model has been developed to a represent friction-involved vibration system. This model incorporates the representation of contact friction using a Jenkins element, accounting for stick, slip, and separation motions occurring at the friction interface. The steady-state response of the system is calculated using the Harmonic Balance method with an alternative frequency-time scheme where its results are validated using a time domain solver. A parametric study is then conducted to examine the mutual relationship between the frictional and vibrational behaviour such as excitation level, contact stiffness, normal load, coefficient of friction, dynamic response, and the effects of vibration on friction force through a newly introduced quantity called equivalent stiffness.

1. Introduction

Friction is the resistance encountered when two objects move relative to each other. It is the result of the molecular interaction between the surfaces in contact this resistance to motion. Friction can serve as a damping mechanism through relative motion between contacting surfaces, like joints or friction dampers in turbomachinery, to disperse vibration energy and therefore reduce vibrations. Friction and vibration represent two fundamental aspects of mechanical systems that significantly influence each other's behaviour [1]. Understanding the mutual effects between friction and vibration is paramount for optimizing the performance, reliability, and efficiency of various engineering systems, ranging from industrial machinery to transportation vehicles. This study focuses on the interaction of a friction-involved vibration system such as joints and friction dumpers. The nonlinear nature of friction and its implications on vibrating systems were investigated by many studies [2,3]. Friction being a dissipative force, introduces complexities in the dynamic response of mechanical systems, often leading to complex stick-slip motion phenomena e.g., shifting the resonance frequency, increasing the structural damping, and causing amplitude-dependent vibration [4]. Advanced modelling techniques are needed to simulate the complex nonlinear dynamic response of such friction-involved vibrations.

Conversely, applying external periodic force can be used to alter the friction forces. This concept can potentially decrease frictional force that has been recognized since at least the 1950s [5]. The impact of vibrations on frictional behaviour has been explored in [6], showing that vibrations can induce variation

in the friction coefficient at the contact interface, thereby affecting the overall performance of the system. This is particularly relevant in applications where precise control of friction is crucial, such as in manufacturing processes and robotics [7]. In the references [8,9] they provide theoretical direction on how to efficiently reduce friction-induced vibration in a braking system by strategically applying tangential harmonic stimulation. The influence of the vibration in friction was also explored in [10] where they observed that the Coulomb friction is effectively reduced due to the dither effect when a vibrating table is employed. Likewise, in reference [11], they introduce the so-called micro-walking machine to examine the effects of system dynamics on sliding friction. By employing a consistent external force rather than a harmonic one to control the friction interface, showing that micro-vibrations significantly affect the frictional resistance of the sliding smooth system. The research in [12] performed an experimental study to explore the use of vibration to facilitate the wind turbine decommissioning process through a scaled model of a slip-joint at a ratio of 1:10. The study highlight the significance of choosing an appropriate forcing frequency vibration for the successful installation or dismounting of a slip-join.

However, there are very few theoretical and numerical studies to investigate such mutual effects between friction and vibration due to the complexities in modelling friction and solving nonlinear equations. To numerically investigate it, it is necessary to solve the nonlinear ordinary equations, which include non-smooth contact friction force. Several numerical techniques commonly employed in dynamic simulations comprise the Runge-Kutta method, Newmark-β method, Harmonic Balance method (HBM), central difference method, and various others [13]. Recently, HBM as a numerical technique in the frequency domain have been widely used in engineering applications to solve nonlinear ordinary differential equations (ODEs) [14]. Unlike traditional time-domain methods that simulate the system's behaviour over time, the HBM transforms the motion into the frequency domain using Fourier series to find the steady-state solution of the nonlinear system. This allows for the representation of time-varying dynamic response as a series of sinusoidal components at different frequencies. HBM is especially useful when dealing with systems subjected to periodic forcing. Alternative Frequency Time (AFT) scheme is often employed within HBM framework to evaluate the nonlinear forces [15]. This technique relies on the use of discrete Fourier transformation and inversed discrete Fourier transformation of the system response. At each iteration, it switches the system response from the frequency domain to the time domain through FFT to calculate the nonlinear force, and then transforms these nonlinear terms back to the frequency domain using FFT enabling the iteration on the frequency spectrum of the steady-state response to continue. The effectiveness of the method is shown through its application in solving a problem involving friction damping [16], especially when the excitation includes multiple discrete frequencies, the AFT method offers a versatile solution to efficiently evaluate any type of nonlinear forces, for example, with different contact laws.

The earlier studies show that friction and vibration are interrelated having mutual effects on each other. Understanding and managing their interactions is essential in various fields. The primary contribution of the current work consists in the investigation into the mutual effects between friction and vibration using a generic lumped parametric model where various friction vibration factors and their corresponding effects are assessed. The influence of vibration on the contact friction is also evaluated through the equivalent stiffness for the first time. The structure of this paper is as follows: Section 2 describes the mathematical model to present the friction-involved vibration. Section 3 presents the fundamental knowledge of the numerical methods that are utilized to analyse the mathematical model, also the analysis tools that are used in the present work. Section 4 presents a numerical validation study to validate the Harmonic Balance method against the time domain methods. Sections 5, and 6 describe the parametric studies with respect to the mutual effects between friction and vibration, along with the interplay of various parameters. Finally, Section 7 offers a summary of the principal conclusions and provides recommended suggestions.

2. Modal description: friction-involved vibration

A system with a two-degree-of-freedom exhibiting dry friction nonlinearity, as shown in figure 1, is considered. The system has two spring-connected masses with one of them in contact with the ground.

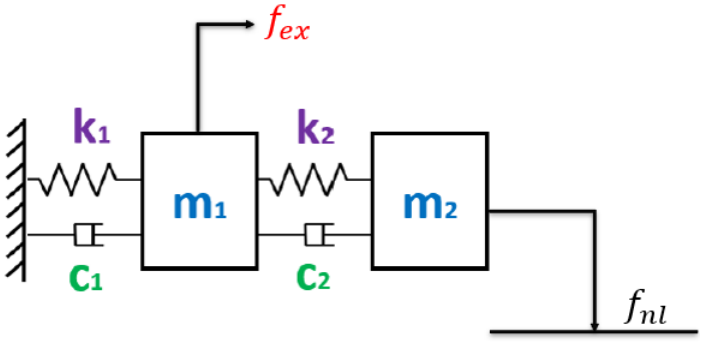

Figure 1. 2-DoF frictional model

The equations of motion of 2-DoF system are expressed as:

$$\begin{bmatrix} m_1 & 0 \\ 0 & m_2 \end{bmatrix} \begin{pmatrix} \ddot{x} \\ \ddot{y} \end{pmatrix} + \begin{bmatrix} c_1 & 0 \\ 0 & c_2 \end{bmatrix} \begin{pmatrix} \dot{x} \\ \dot{y} \end{pmatrix} + \begin{bmatrix} k_1 + k_2 & -k_2 \\ -k_2 & k_2 \end{bmatrix} \begin{pmatrix} x \\ y \end{pmatrix} + \begin{bmatrix} 0 \\ f_{nl} \end{bmatrix} = \begin{bmatrix} f_{ex} \\ 0 \end{bmatrix} \quad (1)$$

Where m_1 and m_2 represent the masses of the first and second components, c_1 and c_2 denote the damping coefficients corresponding to the first and second components, and $k_1$and k_2 represent the tangential contact stiffness for the first and second masses, respectively. f_{nl} stands for the nonlinear friction force modelled by the Jenkins element to depict the stick, slip, and separation motions occurring on the friction interface. The details of the Jenkins element will be described in the next subsection. f_{ex} is the external excitation force for this model, which is expressed as $f_{ex}(t) = A\cos(\omega t)$ where A the excitation force amplitude and ω the excitation force frequency.

2.1 Jenkins element model

The nonlinear force on friction interface is computed through the Jenkins element [17], which is based on the elastic Coulomb's law. Its expression is described in the equation (2) as follows:

$$f_{nl}(t) = \begin{cases} k_t \times \big(x(t) - z(t)\big) & if \ \ |k_t(x(t) - z(t))| \le \mu N_0 \ (Sticking) \\ \mu N_0 \times \big(sign(\dot{z}(t)\big) & if \ \ |k_t(x(t) - z(t))| > \mu N_0 \ \ (Sliding) \end{cases} \quad (2)$$

Where x stands for the relative tangential displacement between interfaces, and z is internal variable for sliding position. k_t is tangential stiffness and $N_0$is the normal load. The contact friction force depends on the contact conditions. When the friction force between the surfaces is below the friction limit of μN, the contact condition is in the sticking phase. Once the friction force surpasses this limit, the surfaces begin to slide.

Figure 2 shows the hysteresis loop of this Jenkins element including the sticking and sliding conditions. Hysteresis loop is commonly used to manifest the dissipation of the energy in mechanical and structural systems. During the sticking condition, the contact force is proportional to displacement. Once the contact force reaches the friction limit, the contact surface starts to slide, and the nonlinear force keeps constant as μN, opposing to the direction of the sliding velocity.

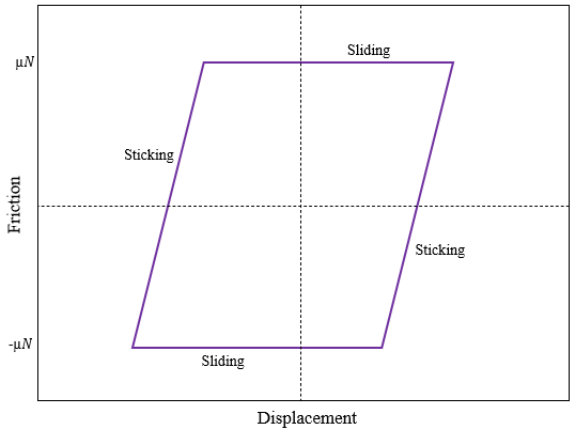

Figure 2. Hysteresis loop

3. Methodology: The Harmonic Balance and Runge-Kutta methods

To calculate dynamic responses of nonlinear ordinary differential equations (ODEs) as shown in equation (2), both Harmonic Balance method and Runge-Kutta methods is used to solve the equation in this study. The details of each method will be briefly introduced in the following.

3.1 Harmonic Balance method

The principle of HBM is to approximate the steady state periodic or quasi-periodic solution using a truncated Fourier series. The equations are derived by setting up the governing equations of motion for the system and assuming a solution of the form:

$$x(t) = \sum_{n}^{N} A_{n,c} cos\ (n\omega t) + A_{n,s} \sin\ (n\omega t) \tag{3}$$

where $x(t)$ is the periodic solution, $A_{n,c}$and $A_{n,s}$are the amplitude of the sin and cos function of the n^{th} harmonic part, ω is the fundamental frequency, and N is the number of harmonics considered in the analysis. The coefficients A_n can be determined by substituting the assumed solution in equation (2) into the governing equation to solve the linear algebra equations for these coefficients. Employing the AFT scheme, it seamlessly transitions between the frequency and time domains for the calculation of nonlinear forces. As depicted in figure 3, the nonlinear force f_{nl} is computed using an iterative scheme that alternates between the frequency and time domains. Various calculations are conducted in different domains within the AFT scheme. It is important to note that this method can only be applied under the assumption that both the solution and the nonlinear force are periodic. The numerical continuation method using predictor-corrector scheme as described by [18] is used to track their solutions as parameters change, which can effectively simulate the softening or hardening nonlinear response. Initially, an estimation of the solution path is made, predicting the next point based on known information. This estimation is refined through more correct calculations, improving the accuracy of the solution with each iteration until convergence toward the actual solution or path. These combined numerical techniques are especially useful for solving nonlinear systems and understand how their behaviour alters with parameter variations. The HBM framework can incrementally adjust a parameter to compute solutions at each step.

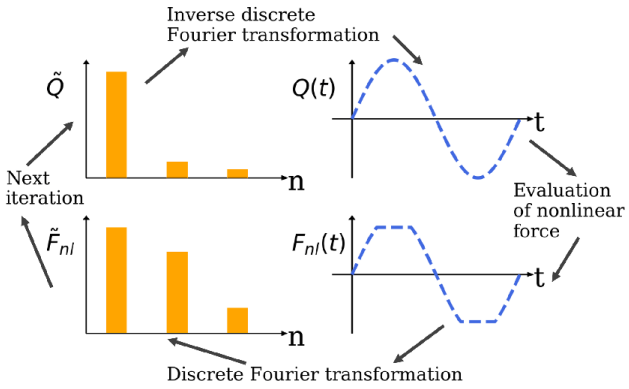

Figure 3. Dynamic response through frequency/time domain analysis [19]

3.2 Runge-Kutta method

The Runge-Kutta method [20] is a numerical technique for solving ordinary differential equations (ODEs) in many fields. It starts by initializing with an initial condition. Then, it proceeds through incremental steps, where the function's value is updated at each step using a predetermined step size. At each step, slopes are estimated by evaluating the function at intermediate points. These slopes are combined to calculate a weighted average, determining the overall slope for the interval. Using this slope, the function value is updated, and the process repeats until reaching the desired endpoint. It provides an approximate numerical solution of the general ODE equation especially helpful when analytical methods are not possible such as the system including non-smooth functions. In this work, the method will be used to validate the results obtained from the HBM.

4. Numerical validation

In this section, the dynamic behaviour of the system, as depicted in figure 1, has been analysed using both HBM and time domain method. The dynamic responses obtained from frequency domain analysis (FDA) are compared to time domain analysis (TDA) for validation. Table 1 shows the specific parameters of the dynamic system depicted in figure 1 for the numerical study.

Table 1. The constant system parameters for the frictional model with 2-degree-of-freedom

k_1 (N/m)	k_2 (N/m)	c_1 (Ns/m)	c_2 (Ns/m)	m_1 (kg)	m_2 (kg)	μ	k_t (N/m)	N_0 (N)	f_{ex} (N)
1	0.5	0.1	0.1	1	1	0.02	0.2	1	0.4

Figure 4 depicts the dynamic response obtained through FDA, whereas figure 5 presents the results obtained using TDA. In Figure 4, two resonances of the system are depicted, located at frequencies of 0.5 rad/sec and 1.3 rad/sec in the frequency domain, at which the system experiences the largest dynamic responses.

In comparison to the time domain solution shown in figure 5, the relative error of the second resonance amplitude between frequency domain analysis and time domain analysis is 2% for $m1$ and 3.4% for $m2$ respectively. Figure 6 shows the comparison of the hysteresis loop from the frequency and time domain solution at the excitation frequency $\omega = 0.5\, rad/sec$. The friction force varies between the friction limit ± 0.02, which is corresponding to static friction force value $f_s = \mu N$. It is found that the error in dissipated energy between frequency domain analysis and time domain analysis is 1.8%. This small error from the dynamic response as well as that in hysteresis loop valid the use of the HBM for the following parametric study in an efficient way.

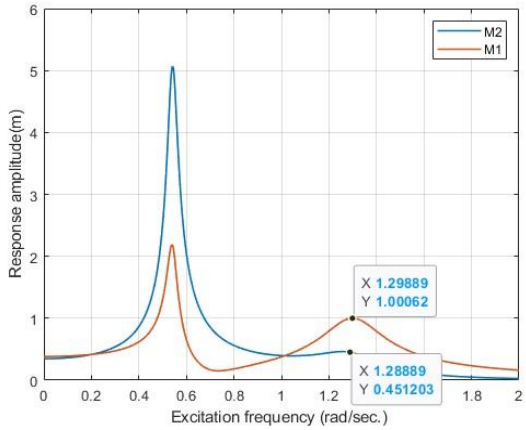

Figure 4. Dynamic response through frequency domain analysis

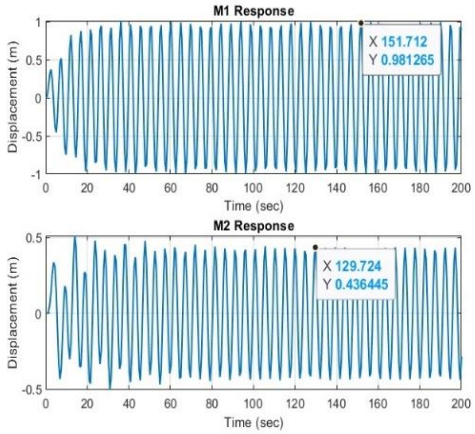

Figure 5. Dynamic response through time domain analysis

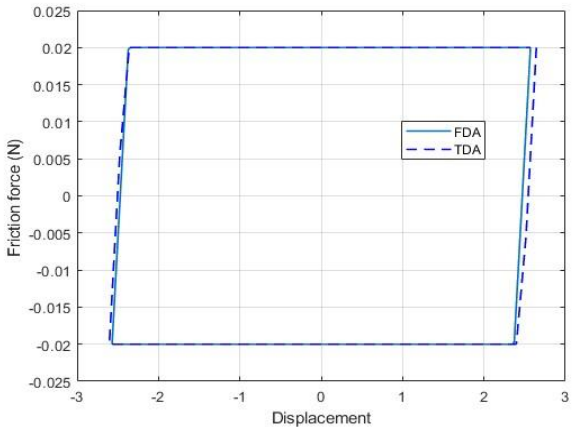

Figure 6. Hysteresis loop dynamics- time and frequency domain analysis $m_2\ at\ \omega = 0.5\ rad/\sec and\ f_{ex} = 0.4\ N$

5. The effects of friction on vibration

Figure 7 illustrates the nonlinear dynamic response of the system at different applied force levels. The hysteresis loops at the first resonance of the nonlinear dynamical response different excitation levels are plotted in figure 8. Figure 7 shows that before the friction force surpasses the friction limit $0.2\ N$, the reception stays constant as there is no energy dissipation on the friction interface. With further increments in the applied excitation force, the reception starts to decline due to the energy dissipation from the sliding friction interfaces. There is also a noticeable decrease in resonance frequency due to the softening effect induced by the slipping on the friction interface. When $A = 0.2\ N$, the ratio of the energy dissipation and energy input reaches the maximum leading to minimum reception in the nonlinear dynamical response as shown in figure 7. This ratio will increase with a further increase in the excitation level contributing to the following increase in the reception.

As can be seen in figure 8, the excitation level directly influences the contact condition, leading to a softening effect characterized by an increased slipping phase. At low excitation levels e.g., $A = 0.002\ N$, the contact between two surfaces is in a sticking condition, leading to a relatively stiff contact interface and no energy dissipation on the friction interface. A further increase in force amplitude makes the friction force between surfaces generally approach the friction limit. Once the friction force reaches

this critical point, the friction interface transits into a sliding condition, leading to a decrease in the effective stiffness of the contact interface and an increase in energy dissipation.

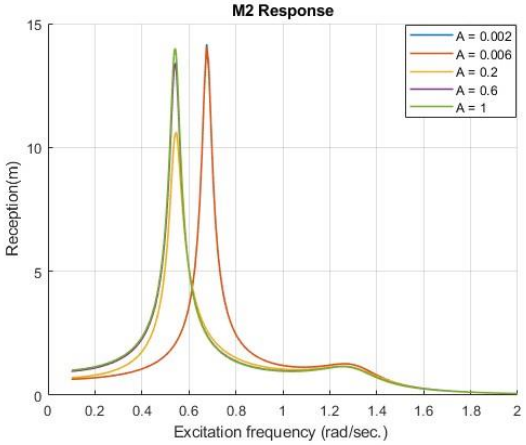

Figure 7. Dynamic response variations with different external force amplitudes A

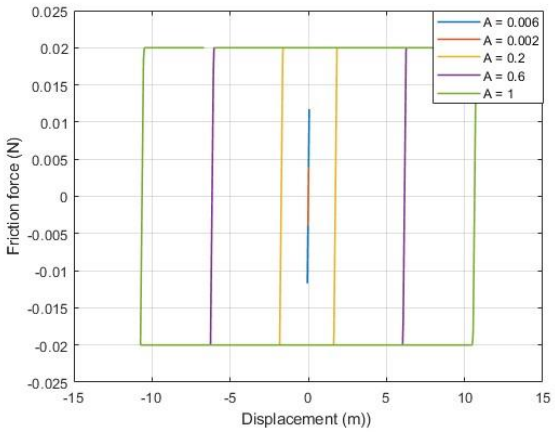

Figure 8. Hysteresis loop evolution with varying excitation level A

Figure 9 shows the changes in dynamic response corresponding to the variation in the coefficient of friction. The hysteresis loop of the first resonance in nonlinear dynamic response is described in figure 10. As shown in figure 10, it is obvious that the friction limit increases with the coefficient of friction, leading to an increasing presence of sticking phases in the hysteresis loop while a decreasing sliding distance. It leads to an increase in interface stiffness until it reaches the full sticking phase. These combined effects also make the energy dissipation increase from μ = 0.01 to μ = 0.06 and then decrease to zero when the μ increases to 0.3. For the fixed excitation level A, the reception as shown in figure 9 initially decreases as energy dissipation increases. After reaching a critical coefficient of friction $\mu =$ 0.1, the system starts to transit into a full sticking phase, causing energy dissipation to decline as shown in figure 10, as a result, the reception starts to increase as shown in figure 9. As the increase of coefficient of friction, the stiffness of the friction interface increases due to the decreasing sliding regime on the

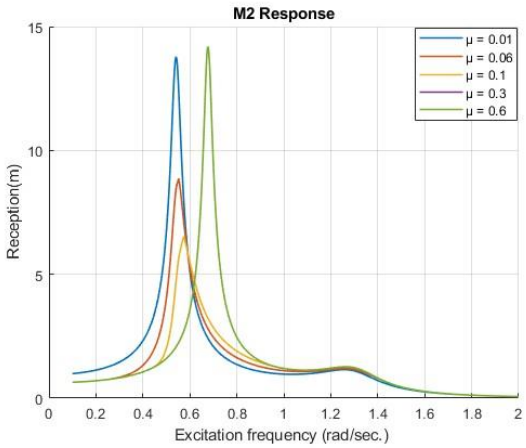

Figure 9. Dynamic response variations with different coefficient of friction μ

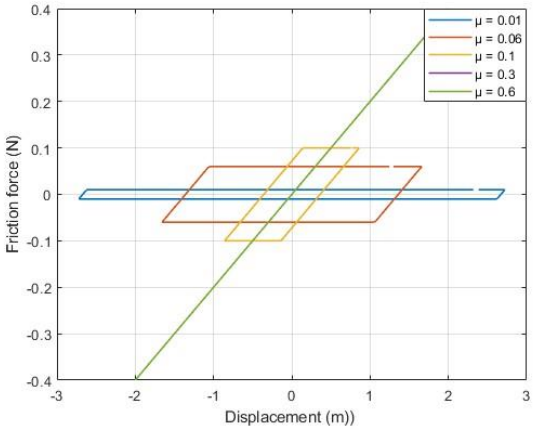

Figure 10. Hysteresis loop evolution with varying coefficient of friction μ

hysteresis loop, until it reaches its maximum value (contact interface stiffness k_t). When coefficient of friction reaches 0.3. This is accounted for the increase in resonance frequency at the beginning until the full sticking phase is reached.

6. The effects of vibration on friction

A parameter called "equivalent stiffness" is introduced to assess the impact of vibration on the friction force exerted on the surface. The equivalent stiffness is defined as the slope between points A, and B as shown in figure 11. The equivalent stiffness illustrates the softening effects on the interface indicating the stiffness between friction interfaces. The maximum equivalent stiffness equals the contact interface stiffness k_t occurring when the interface is fully stuck with zero energy dissipated due to friction, while the equivalent stiffness decreases when the interface experiences sliding between surfaces starting to dissipate the vibration energy.

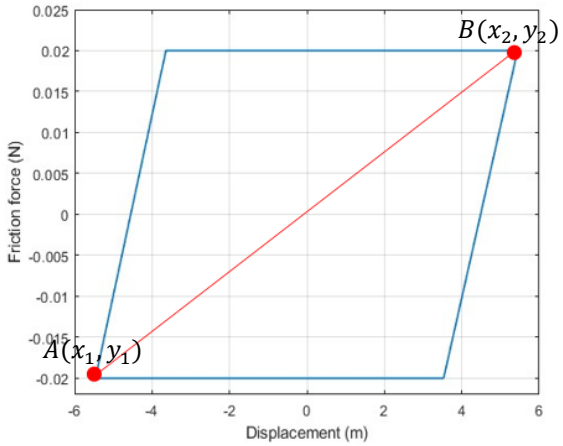

Figure 11. Hysteresis loop

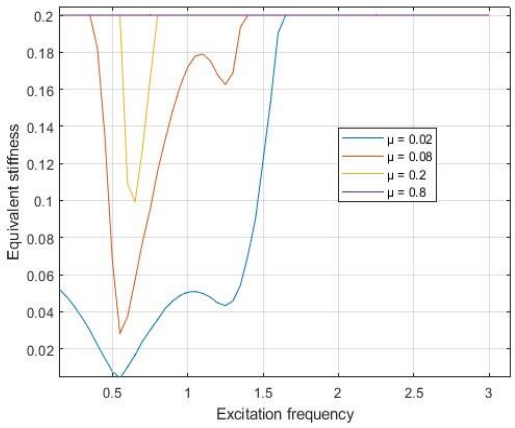

Figure 12. Equivalent stiffness across different friction coefficients at $A = 0.4\ N$

In Figure 12, the variation of equivalent stiffness with the rise in coefficient of friction is depicted. For each curve, a decline in equivalent stiffness is seen when the excitation frequency approaches the first resonance frequency for each curve, where the system exhibits the highest energy dissipation. Following that, with an increase in excitation frequency, the equivalent stiffness increases until the system reaches the second resonance where the equivalent stiffness declines again. After the applied excitation frequency surpasses the second resonance, the equivalent stiffness starts to increase again with increasing excitation frequency. This trend stays until the equivalent stiffness matches the surface contact stiffness, where the contact is fully stuck and there is no energy dissipation in the system. As the coefficient of friction rises, the stiffness of the friction interface increases owing to the reduction in the sliding regime observed on the hysteresis loop, until it reaches its maximum value, denoted as the contact interface stiffness. This phenomenon holds significance in scenarios where the required equivalent stiffness needs to be minimal to initiate separation or sliding between the interacting surfaces e.g., joint connections.

Figure 13 illustrates the impact of changing excitation force amplitude on the equivalent stiffness. With increasing amplitude of the excitation force, the equivalent stiffness decreases further over the frequency. This observation aligns with the findings from figures 7 and 8, which show that the increase in excitation force amplitude affects the contact condition, resulting in a softening effect. This, in turn, leads to a decrease in equivalent stiffness. For each plot, it is seen that when the excitation force frequency at a system resonance of $0.6\ rad/sec$, it results in the lowest equivalent stiffness. This occurs because the system generates the widest hysteresis loop, coupled with the highest energy dissipation, leading to the lowest slope. Conversely, when the excitation force frequency is far from resonances, the equivalent stiffness increases due to a decrease in energy dissipation. Until the applied excitation frequency matches the second resonance of the system at $1.3\ rad/sec$, where the equivalent stiffness declines again, and then starts to increase. With further increases in the applied frequency, the contact becomes fully stuck, at this point, the equivalent stiffness reflects the system's contact stiffness, resulting in linear dynamical behaviour.

Figure 14 shows the impact of varying contact stiffness on the equivalent stiffness in the frequency dynamical response. It shows an increase in excitation frequency has no effect on equivalent stiffness for different contact stiffness values until a specific frequency around $\omega = 1.3\ rad/sec$ is reached. At this frequency, for each curve, there is a noticeable increase in equivalent stiffness until it reaches its maximum value, which is equal to the contact stiffness of the interface. Afterwards, the equivalent stiffness stays constant. It is because at low excitation frequency with large hysteresis loops, the slope is primarily influenced by the sliding distance. However, at high excitation frequency with smaller hysteresis loops, the slope is more affected by the contact stiffness.

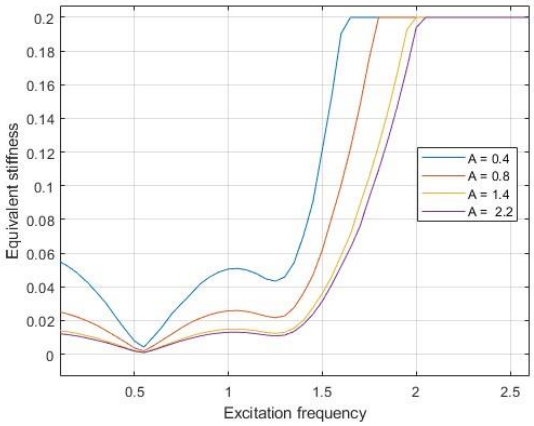

Figure 13. Correlation between excitation frequency and equivalent stiffness at $A = 0.4\ N$

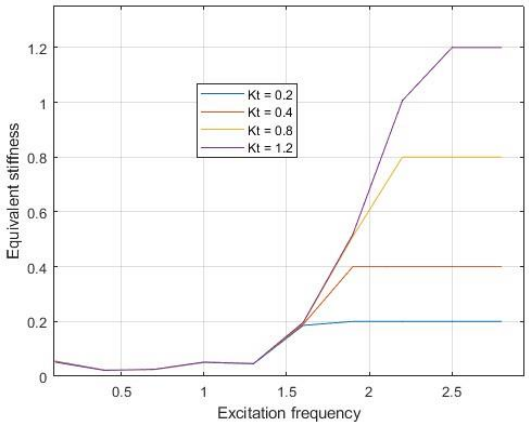

Figure 14. Variations in equivalent stiffness across different contact stiffness at $A = 0.4\ N$

7. Conclusion

In summary, a 2-degree-of-freedom lumped parameter model, incorporating the Jenkins element model, was developed to study the mutual effects between friction and vibration. The dynamic behaviour of the system was analysed using the Harmonic Balance method coupled with an alternative frequency-time scheme. In this study, the frequency response obtained from HBM was validated by the R-K time domain method. The following parametric results show that friction has a complex influence on the nonlinear vibrational response. For instance, the excitation level directly affects contact conditions on the friction interface, leading to transitions between sticking and slipping phases, changes in effective interface stiffness, and variations in energy dissipation. This insight is invaluable for mechanical engineers designing systems where friction plays a crucial role, such as automotive components, machinery, and aerospace structures. At low excitation amplitude, the contact between two surfaces is governed by static friction, resulting in a relatively stiff contact interface. In this phase, the surfaces stay in sticking and resist any slipping motion leading to no energy dissipation due to the friction and constant reception in nonlinear dynamic response. As the applied force rises, once the friction limit is reached, the system enters a surface-slipping state leading to a reduction in the effective stiffness of the contact interface and subsequently a decrease in the resonance frequency of the system.

Furthermore, the friction coefficient significantly influences the dynamic response of the system. As the friction limit rises with an increase in the coefficient of friction, the friction interface transitions from a slipping condition to a sticking condition. This transition is accompanied by an increase in energy dissipation followed by a decrease due to the combined effects of reduced sliding distance and increased friction limit. As a result, the nonlinear frequency response initially decreases, and then increases with the increase of coefficient of friction. Consequently, the resonance frequency increases due to the stiffening effect. Understanding how changes in the coefficient of friction affect energy dissipation and resonance frequency can be important for reliable mechanical systems, such as optimizing suspension systems in vehicles to enhance vehicle ride comfort and handling, designing robust aerospace components, and enhancing the performance of industrial machinery. The equivalent stiffness shows its

lowest values at the system's resonance due to the occurrence of the maximum energy dissipation. On the contrary, the highest equivalent stiffness occurs when the interface is fully stuck. Altering the surface stiffness does not change the equivalent stiffness at low frequencies, but it increases the equivalent stiffness at higher frequencies due to smaller sliding distance. This phenomenon is due to the large hysteresis loops at low excitation frequencies, where the slope is primarily influenced by the sliding point while influenced by the contact stiffness at high excitation frequencies with smaller hysteresis loops. By considering the impact of surface stiffness on equivalent stiffness values, engineers can make informed decisions regarding material selection and design parameters to minimize friction-vibration systems and improve overall efficiency. A further investigation will be necessary to explore the multiscale topographies of the contact interface and their impact on various contact characteristics of surfaces, including contact stiffness, pressure distribution, frictional behaviour, and nonlinear dynamic response.

Acknowledgments
Ahmad Algara is grateful for the funding from International Strategic Partner (ISP) programme at the University of Strathclyde. The authors also acknowledge the support from Dr Alessandro Cabboi at Delft University of Technology, Netherland for beneficial feedback throughout this study.

References

1. Yuan J, Salles L, Schwingshackl C. Effects of the geometry of friction interfaces on the nonlinear dynamics of jointed structure. InNonlinear Structures & Systems, Volume 1: Proceedings of the 39th IMAC, A Conference and Exposition on Structural Dynamics 2021 2022 (pp. 67-74). Springer International Publishing.
2. Thompson JM, Stewart HB, Turner R. Nonlinear dynamics and chaos. Computers in Physics. 1990 Sep;4(5):562-3.
3. Hinrichs N, Oestreich M, Popp K. Dynamics of oscillators with impact and friction. Chaos, Solitons & Fractals. 1997 Apr 1;8(4):535-58.
4. Artiles AF. The Effects of Friction in Axial Splines on Rotor System Stability. InTurbo Expo: Power for Land, Sea, and Air 1991 Jun 3 (Vol. 79023, p. V005T14A043). American Society of Mechanical Engineers.
5. Fridman HD, Levesque P. Reduction of static friction by sonic vibrations. Journal of applied physics. 1959 Oct;30(10):1572-5.
6. Lu J, Zhao Z. Effect of Interface Tangential Relative Motion Caused by Vibration on Friction. Beijing Da Xue Xue Bao. 2020;56(5):777-84.
7. Sfakiotakis M, Pateromichelakis N, Tsakiris DP. Vibration-induced frictional reduction in miniature intracorporeal robots. IEEE Transactions on Robotics. 2014;30(5):1210-21.
8. Thomsen JJ. Using fast vibrations to quench friction-induced oscillations. Journal of sound and vibration. 1999 Dec 16;228(5):1079-102.
9. Liu N, Ouyang H. Suppression of friction-induced-vibration in MDoF systems using tangential harmonic excitation. Meccanica. 2020 Jul;55(7):1525-42.
10. Matunaga S, Onoda J. New gravity compensation method by dither for low-g simulation. Journal of Spacecraft and Rockets. 1995 Mar;32(2):364-9.
11. Wetter R, Popov VL. The influence of system dynamics on the frictional resistance: insights from a discrete model. Tribology Letters. 2016 Feb;61:1-20.
12. Cabboi A, Segeren M, Hendrikse H, Metrikine A. Vibration-assisted installation and decommissioning of a slip-joint. Engineering Structures. 2020 Apr 15;209:109949.
13. Rao SS. Vibration of continuous systems. John Wiley & Sons; 2019 Mar 6.
14. Razzak MA. A simple harmonic balance method for solving strongly nonlinear oscillators. Journal of the Association of Arab Universities for Basic and Applied Sciences. 2016;21:68-76.

15. Zhang ZY, Chen YS. Harmonic balance method with alternating frequency/time domain technique for nonlinear dynamical system with fractional exponential. Applied Mathematics and Mechanics. 2014 Apr;35(4):423-36.
16. Sanliturk K, Ewins D. Modelling two-dimensional friction contact and its application using harmonic balance method. Journal of sound and vibration. 1996;193(2):511-23.
17. Singer IL, Pollock H, editors. Fundamentals of friction: macroscopic and microscopic processes. Springer Science & Business Media; 2012 Dec 6.
18. Umbría JS, Net M. Numerical continuation methods for large-scale dissipative dynamical systems. The European Physical Journal Special Topics. 2016 Nov;225(13-14):2465-86.
19. Sun Y, Yuan J, Vizzaccaro A, Salles L. Comparison of different methodologies for the computation of damped nonlinear normal modes and resonance prediction of systems with non-conservative nonlinearities. Nonlinear Dynamics. 2021 Jun;104(4):3077-107.
20. Butcher JC. A history of Runge-Kutta methods. Applied numerical mathematics. 1996;20(3):247-60.
21. Chen F, Ouyang H, Wang X. A new mechanism for friction-induced vibration and noise. Friction. 2023 Feb;11(2):302-15.
22. Fidlin A. Nonlinear oscillations in mechanical engineering. Springer Science & Business Media; 2005 Dec 19.